Journal of the Korean Society of Oceanography
Vol. 34, No. 2, pp. 73—85, June 1999

A Three-Dimensional Numerical Study of Effects of Typhoons on Oceanographic Conditions in the Korea Strait

CHUL-HOON HONG
Research Center for Ocean Industrial Development, Pukyong National University, Pusan 608-737, Korea

When typhoons passed around the Korea Strait, some observation in this strait carried out by Mizuno *et al.* (1986) gives us the following oceanographic features; 1) the direction of the observed current was opposite to the northeasterly wind, 2) temperature rapidly increased having a time lag as the depth deepens, after then decreased with oscillation. A primitive equation ocean model that makes use of a sigma-coordinate system and incorporates a typhoon model was used to examine the mechanism to generate these phenomena. The model region covers the East China Sea, the Yellow Sea, and a portion of the East Sea (Japan Sea). The model well reproduces the observed features, especially in temperature field, and clearly manifests how the above observed features happened. From early time when the typhoon was located in low latitude, an alongshore northward current in the west of Kyushu (hereafter the West Kyushu Current) is generated by an alongshore wind in the typhoon. This current flows into the eastern channel, as a coastal jet, regardless to the wind field within the Korea Strait during this period. The above observed phenomena are generated by this current. The model results indicate that when typhoons pass around the Korea Strait, the West Kyushu Current is generated, and oceanographic condition in the strait should be greatly influenced by this current.

INTRODUCTION

Every year many typhoons from tropical regions pass around the Korea Strait (henceforth KS; Fig. 1), and seriously influence oceanographic conditions in the KS, even though such typhoons are short-term impacts for several days. Yi (1974) reported the existence of a rapid sea level variation between Izuhara and Pusan when typhoons pass around the KS, and Hong and Yoon (1992) (henceforth HY) examined how such a sea level variation happens using a numerical shallow water model. A disturbance propagation excited by a typhoon through the KS was investigated by Hong and Yoon (1993) in the northern Japanese coast of the East Sea (Japan Sea).

Fig. 2 shows time series of the observed velocity and temperature at St. T4 (see Fig. 1) in the eastern channel of the KS observed by Mizuno *et al.* (1986). Atmospheric pressure and wind speed (upper panels) were obtained from a marine tower of Kyushu University in Japan. Tidal and higher frequency fluctuations were removed by using a low-pass filters. In the observation period, a typhoon (TP8305), of which track is illustrated in Fig. 1, passed the south of Japan during August 15 to 18, 1983. The vertical bar represents a time when TP8305 passed a proximity of the KS. Even though the typhoon has passed far away from the KS, it made there a great impact on oceanographic condition because its scale was very large, e.g., the lowest central pressure was about 890 hpa. In this period, the observed wind direction was basically northeasterly over 10 m/s.

In this observation results, we can point out several oceanographic features. Firstly, the current at St. T4 was northeastward flowing into the East Sea opposing to the wind direction. Moreover, at three layers (50 m, 80 m, and 110 m), the situation is almost the same, implying that the current is basically barotropic. It is not easy to simply understand these results since the current primarily flows downwind. Excluding the mean current speed (about 25 cm/s) in the observed period, variation of velocity by the typhoon can be roughly estimated as about 20 to 40 cm/s. On the other hand, in this period, the temperature (lower panel) rapidly increases, especially higher (3 to 5°C) in the middle layers (50 m and 80 m). The temperature maximum (cross mark) appears earlier in the surface, and delays as the depth deepens. Thus, its time lag between the

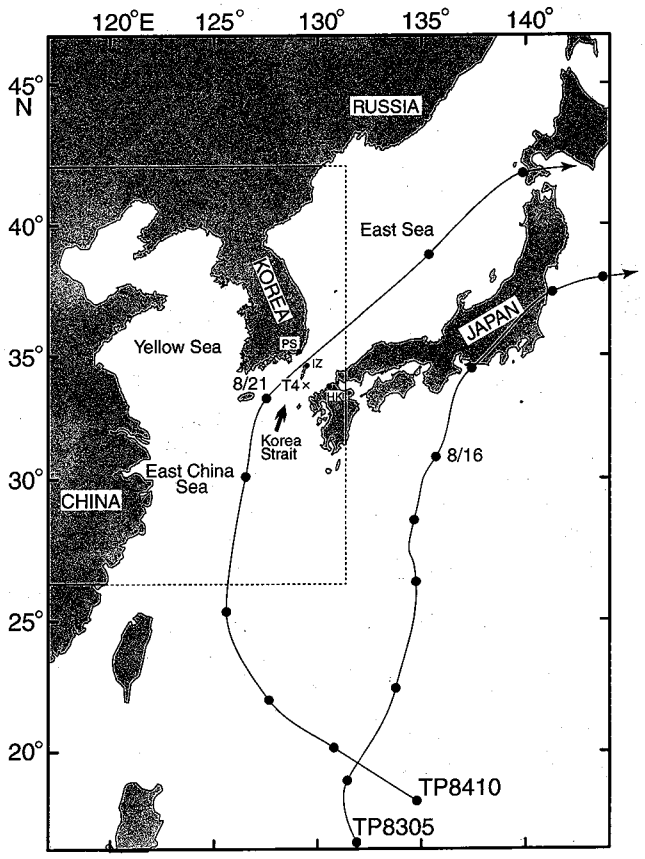

Fig. 1. Map of the Northwest Pacific Ocean area. Tracks of typhoons, (TP8305 and TP8410) are roughly given, and time intervals between black circles on the tracks are one day. Time series of the observed temperature and velocity have been obtained at St. T4 by Mizuno *et al.* (1986). Pusan, Izuhara, and Hakata are symbolized by PS, IZ, and HK, respectively. The model region is indicated by a rectangle, and the dashed lines show open boundaries in the model.

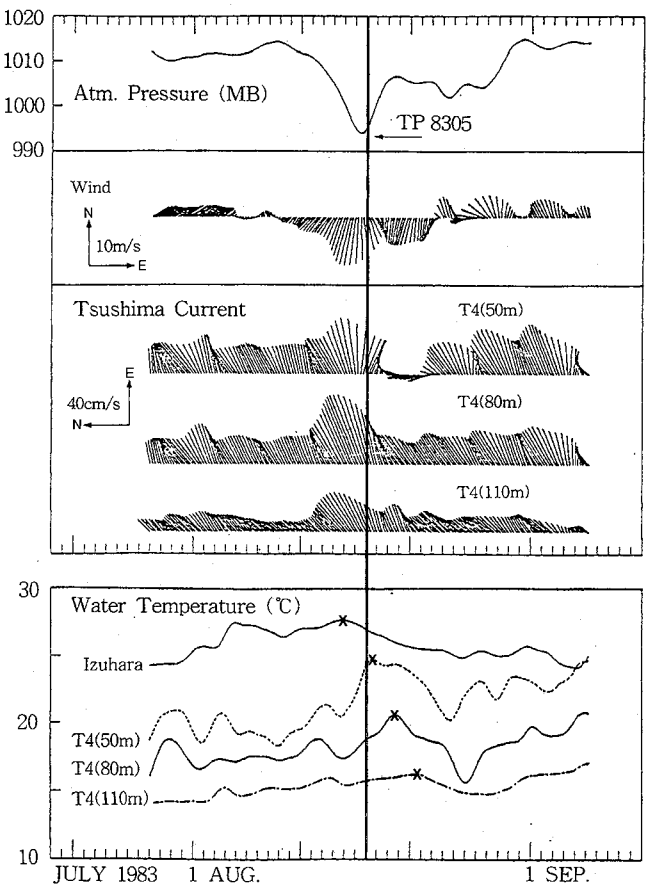

Fig. 2. Time series of velocity and temperature at St. T4 of the eastern channel in August, 1983, with atmospheric pressure and wind speed from a marine tower of Kyushu University in Japan. Data intervals are 6 hours. Reproduced from Mizuno *et al.* (1986). Vertical bar represents a time when TP8305 has passed a proximity to the Korea Strait (KS) on August 16, 1983. Cross marks in the temperature indicate the maximum values.

surface and the bottom layers becomes about 6 to 7 days. After passing of the typhoon, temperature slowly decreases with oscillation for several days.

Another typhoon (TP8410) passed through the KS during August in 1984, as shown in Fig. 1, and velocity and temperature in that period were also observed at St. T4 by Mizuno *et al.* (1986) (Fig. 3). The interval between two vertical bars shows periods of 19th to 23rd, August, when TP8410 passed through the KS. Similar features to those in the case of TP8305 have been also found; the current in the eastern channel flows into the East Sea against to northeasterly wind of the typhoon at least before the typhoon passes through the KS; a rapid increase of temperature also appears, then it decreases with oscillation for several days, and a time lag with the maximum temperature in depth has been found, but it has been shorter (about 2 days) than that of TP8305.

The purpose of this paper is to examine how the above phenomena happen, using a three-dimensional primitive equation model in sigma coordinate.

NUMERICAL MODEL

Governing equations

The ocean model is the Princeton Ocean Model (POM) described in detail by Blumberg and Mellor (1987), and its configurations are almost the same as one used by Hong (1998a). POM has been used by many coastal oceanographers due to being well documented and effectively reproducing coastal and estuarine bodies of water (Blumberg and Mellor, 1983; Galperin and Mellor, 1990a, b; Oey *et al.*,

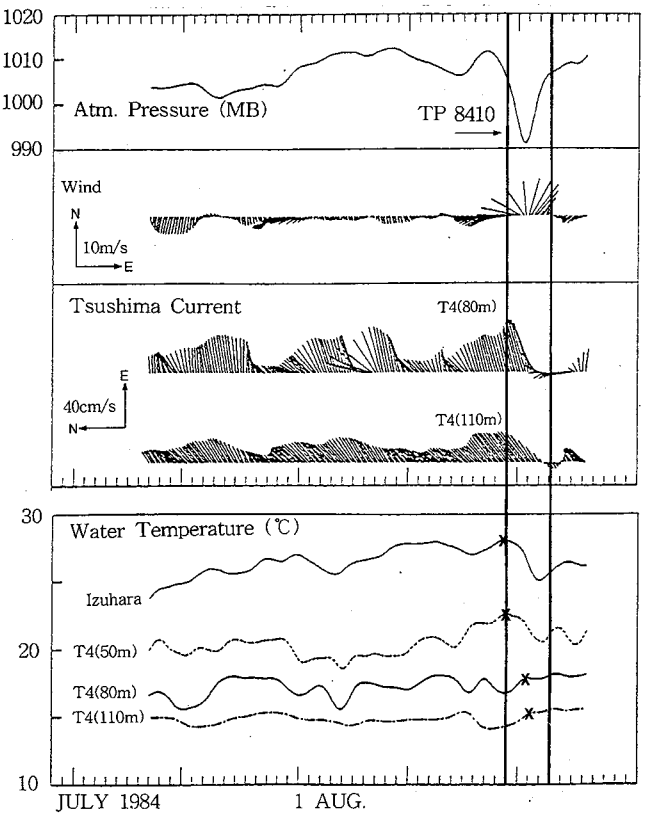

Fig. 3. Same as Fig. 3 except for TP8410. The interval between two vertical bars shows a few-days period of the passing of TP8410 through the KS.

1985a, b, c). Recently, it has been applied to tidal motion in the coastal ocean of Korea (Hong and Choi, 1997; Hong, 1998b), and to circulation in the Yellow Sea and the East China Sea (Oh *et al.*, 1998). It is a primitive equation model with a free surface, a split mode time step, and solves the following traditional hydrodynamic equations for conservation of mass, momentum, temperature, and salinity coupled with the equation of state.

$$\frac{\partial u}{\partial x}+\frac{\partial v}{\partial y}+\frac{\partial w}{\partial z}=0 \tag{1}$$

$$\frac{\partial u}{\partial t}+u\frac{\partial u}{\partial x}+v\frac{\partial u}{\partial y}+w\frac{\partial u}{\partial z}-fv = -\rho_0^{-1}\frac{\partial p}{\partial x}+\frac{\partial}{\partial z}\left(K_M\frac{\partial u}{\partial z}\right)+F^x \tag{2}$$

$$\frac{\partial v}{\partial t}+u\frac{\partial v}{\partial x}+v\frac{\partial v}{\partial y}+w\frac{\partial v}{\partial z}+fu = -\rho_0^{-1}\frac{\partial p}{\partial y}+\frac{\partial}{\partial z}\left(K_M\frac{\partial v}{\partial z}\right)+F^y \tag{3}$$

$$\rho g=-\frac{\partial p}{\partial z} \tag{4}$$

$$\frac{\partial T}{\partial t}+u\frac{\partial T}{\partial x}+v\frac{\partial T}{\partial y}+w\frac{\partial T}{\partial z}=\frac{\partial}{\partial z}\left(K_H\frac{\partial T}{\partial z}\right)+F^T \tag{5}$$

$$\frac{\partial S}{\partial t}+u\frac{\partial S}{\partial x}+v\frac{\partial S}{\partial y}+w\frac{\partial S}{\partial z}=\frac{\partial}{\partial z}\left(K_H\frac{\partial S}{\partial z}\right)+F^S \tag{6}$$

$$\rho=\rho(T,S) \tag{7}$$

The notations are conventional: K_M is the vertical eddy viscosity, K_H the vertical eddy diffusivity, $F^{(x,y)}$ the horizontal eddy friction terms, and $F^{(T,S)}$ the horizontal eddy diffusion terms. The Boussinesq and hydrostatic approximations are assumed, and the Knudsen's equation is used to solve the equation (7). The K_M, K_H are determined by Mellor and Yamada level 2.5 turbulence closure model (Galperin *et al.*, 1988). The horizontal friction and diffusion terms are treated by the Laplacian forms with the coefficients A_M and A_H calculated with Smagorinsky scheme. The detailed description for the governing equations is given in Mellor (1996). The model uses a bottom-following, sigma-coordinate system $\sigma=(z-\eta)/(H+\eta)$, where η and H are the sea surface elevation and the water depth, respectively. The model has 12 vertical sigma levels (0.000, −0.016, −0.031, −0.063, −0.125, −0.250, −0.375, −0.500, −0.625, −0.750, −0.875, −1.000).

The model geometry (Fig. 4a), obtained from NOAA National Date Center, is realistic with open boundaries in the east and south (see Fig. 1), and has horizontal resolution of 20 km in both x and y directions from its left-southernmost grid point (26° 00'N, 117°25'E) to its right-northernmost grid point (42°00'N, 132°00'E). The model region covers the East China Sea, the Yellow Sea, and a portion of the East Sea, and an enlarged area of the KS is shown in Fig. 4b. The bottom topography has a maximum depth of 3000 m and has been smoothed so that the sigma coordinate system does not cause spurious current in the region of steep topographic gradients. The model is formulated by a Cartesian coordinate where a shape of typhoon at high latitude should be somewhat deformed owing to curvature variation of the Earth's surface. However, it would not significantly influence the objective of this paper because we mainly focus on phenomenon in the KS (about 35°N) before a typhoon enters the East Sea.

At open boundary the internal normal velocities are governed by a Sommerfeld radiation condition; an elevation is specified as the external open boundary condition. A constant structure of temperature is upwinded on the boundary; when the flow is into

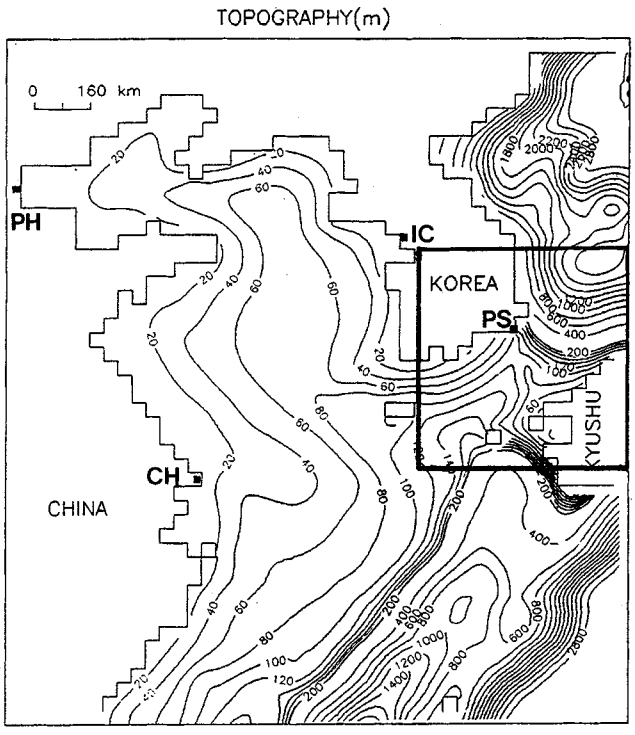

(a)

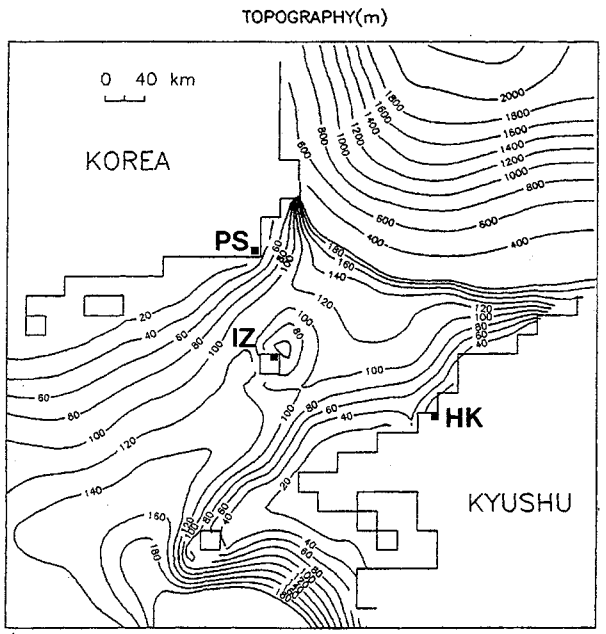

(b)

Fig. 4. Model bathymetry (depths in meters) a). Black rectangles represent stations for drawing a space-time diagram. An enlarged area of the KS b).

the model domain temperature is prescribed, and tangential velocities are subject to free slip condition. The model is initialized with horizontally homogeneous temperature which is exponentially decreased from 27°C at the surface, and the sea level and velocities are set to be zero, $u=v=w=\eta=0$. Salinity distribution, for convenience, is assumed to be equal everywhere to 34.50‰. For simplicity, no heat flux and no basic current, such as the Tsushima current, are considered. The latter may be critical for the model results because the Tsushima Current becomes stronger in the eastern channel during summer. This will be more discussed at the last section. Refer to Hong (1998a) for details of the model.

Atmospheric conditions

Atmospheric conditions in the present study is almost the same as one in Hong (1998a) except for the run-time being from 2100 GMT 17 August, 1984 (hereafter 17:2100) to 27:2100. Briefly repeating some salient points, the air pressure $P(x, y)$ at (x, y) of which the lowest is the center of a typhoon, is given by Fujita (1952),

$$P(x,y)=P_{\infty}-\delta P/\sqrt{1+(r/r_o)^2}$$

where P_{∞} is the ambient air pressure, δP a depression of the air pressure at the center of the typhoon, r the radius from the center of the typhoon, r_0 a distance in which the depression of the air pressure becomes $\delta P/\sqrt{2}$ having the maximum gradient wind, i.e. it corresponds to a radius of the typhoon's core. The isostatic elevation is obtained by hydrostatic equation using the second term in the right hand side of the above equation, and is incorporated in the pressure gradient terms in equations (2), (3).

The wind is given by Miyazaki *et al.* (1961),

$$W=C_g W_g(r)+C_b W_b E^{-\alpha r}$$

where (W_g) is a gradient wind, (W_b) wind is proportional to the moving speed of the typhoon, and C_g $(=0.8)$ and $C_b(=0.5)$ are parameters for fitting to the observation, α a coefficient for exponentially decreased amount of W_b from the center of the typhoon. The wind stresses (τ^x, τ^y) are calculated by

$$(\tau^x, \tau^y)=\rho_a C_d W(w_x, w_y)$$

where C_d $(=2.6\times10^{-3})$ is a drag coefficient of the wind, ρ_a is the atmospheric density, and w_x and w_y are the components of W in x and y directions, respectively. The life of the typhoon was approximately 15 days, but the calculation was done for 10 days from 17:2100 until being a weak cyclone in the Okhotsk Sea. The detailed track of TP8410 used here is illustrated by Fig. 5.

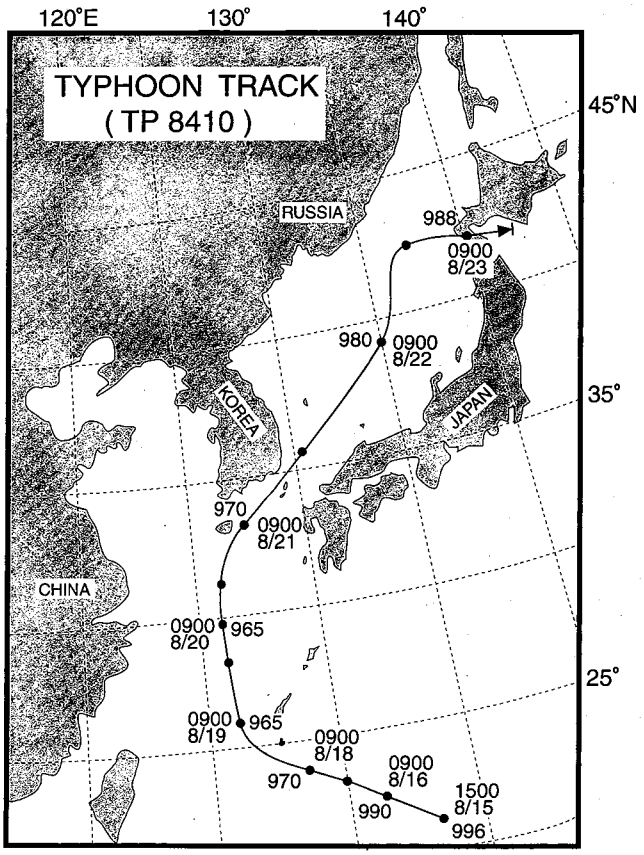

Fig. 5. The track of typhoon TP8410. Filled circles (●) indicate the central position, and the numerals give the central pressure and arrival time for each location.

MODEL RESULTS

Comparison with the observation

Fig. 6 shows time series of the calculated wind (Fig. 6a), velocity (Fig. 6b), and temperature (Fig. 6c) at St. T4 (see Fig. 1). The interval between vertical bars represents twelve hours with passing of the typhoon through the KS. In the model the wind direction before the typhoon passed through the KS is basically easterly, and is slightly different from the observation on the northeasterly wind (Fig. 3). As the typhoon passes through the KS, however, the model wind has been changed to southeasterly and southwesterly winds as the observation. However, it is roughly about two times stronger than the observation (about 10 m/s), probably associated with a limitation of the typhoon model, as already discussed by Hong (1996). On the other hand, the calculated currents in 85 m and 119 m depths at St. T4 (Fig. 6b) are northwestward or northward in the period of the typhoon passing through the KS although the observed current (Fig. 3) was northeastward (note that the compared depths are a little different each other). The current speed is stronger (about two times) than the observation. In the model, after the passing of typhoon through the KS, inertial oscillation with a period of about 22-hour is predominant.

In the temperature field (Fig. 6c), it seems that the observed features (Fig. 3) is rather successfully reproduced; temperature rapidly increases, after then decreases with oscillation for several days; it earlier reaches the maximum level (cross mark) in the surface, and delays as the depth deepens, but the time lag between the surface and the near-bottom is slightly shorter (12 hours) than that in the observation (1.5 to 2 days), probably relating to the overestimated current speed in the model.

Response of open ocean to typhoon TP8410

Fig. 7 shows the sea surface elevation (Fig. 7a), wind vector (Fig. 7b) from 20:0900 to 21:0900 with every twelve-hour. Shade zones represent negative values of the elevations, and the center of the typhoon is marked by a cross symbol (×). The elevation around the center of the typhoon should be basically determined by balancing two effects, i. e., isostatic effect and Ekman effect. The former contributes to increase the sea level due to inverse barometry (hydrostatic equilibrium), and the latter to decrease the sea level due to Ekman divergence. As the typhoon moves on the continental shelf in the East China Sea (20:0900), a cyclonic eddy is formed by Ekman dynamics behind the center of the typhoon, and gradually develops in time. In the Chinese coast (about 30°N; see Fig. 1), sea water is piled up with coastal jet (Fig. 8) developed by the alongshore wind of the typhoon (Fig. 7b), while negative sea level (shade zone) gradually appears in western coastal area of Korean peninsula (21:0900) due to piling-down when the typhoon has closely approached the KS.

In the velocity fields at 20:0900 (Fig. 8a), the cyclonic eddy influences the current field around the KS from early time when the typhoon is located at low latitude, especially in the surface current field (level 3). At this time we note that alongshore-northward current in the west of Kyushu exists although it is more clearly seen at level 3 and 7. Considering the wind field (see the left panel in Fig. 7b), this current is induced by alongshore wind of

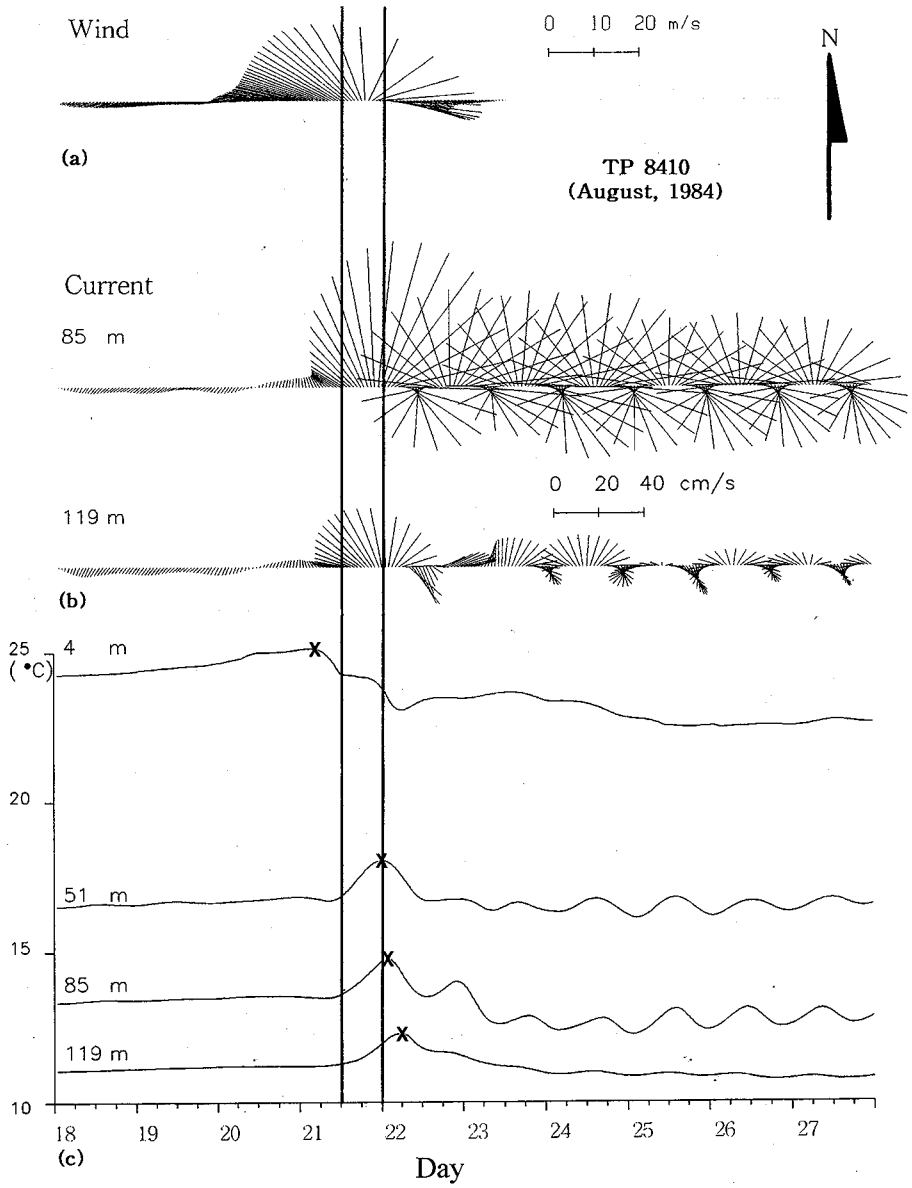

Fig. 6. Time series of the calculated wind a), velocity b), and temperature c) at St. T4 (see Fig. 1). Data intervals are one hour.

the typhoon in the west of Kyushu, as a coastal jet. As the typhoon approaches the KS (21:0900), the current develops more at all layers (Fig. 8b) with stronger alongshore wind in time (see the right panel in Fig. 7b). Therefore, the velocity field accompanied by this current in time governs the current field in the eastern channel in this period, almost regardless of the wind field in the KS. For convenience, hereafter we call it 'West Kyushu Current (WKC)'. This will be discussed more in detail at next section.

One interesting point is that the center of the eddy in the surface layer almost coincides with one of the typhoon, but as the depth deepens, it has been positioned behind the typhoon by about 300 km at near-bottom in this time (Fig. 8b). On the other hand, an interpolated velocity field in z-coordinate at 21:0900 (Fig. 8c) shows that the amplitude is rapidly decreased in depth, for example, at 50 m depth (the middle panel), it has been reduced to about 10 to 20% of the surface one, especially at area out of the eddy. This indicates that the effect of typhoon on the sea water is concentrated on the surface layer.

Response of sea water in the Korea Strait to typhoon TP8410

In this section consider how the observed features (Figs. 2, 3) happened. Fig. 9 shows temperature

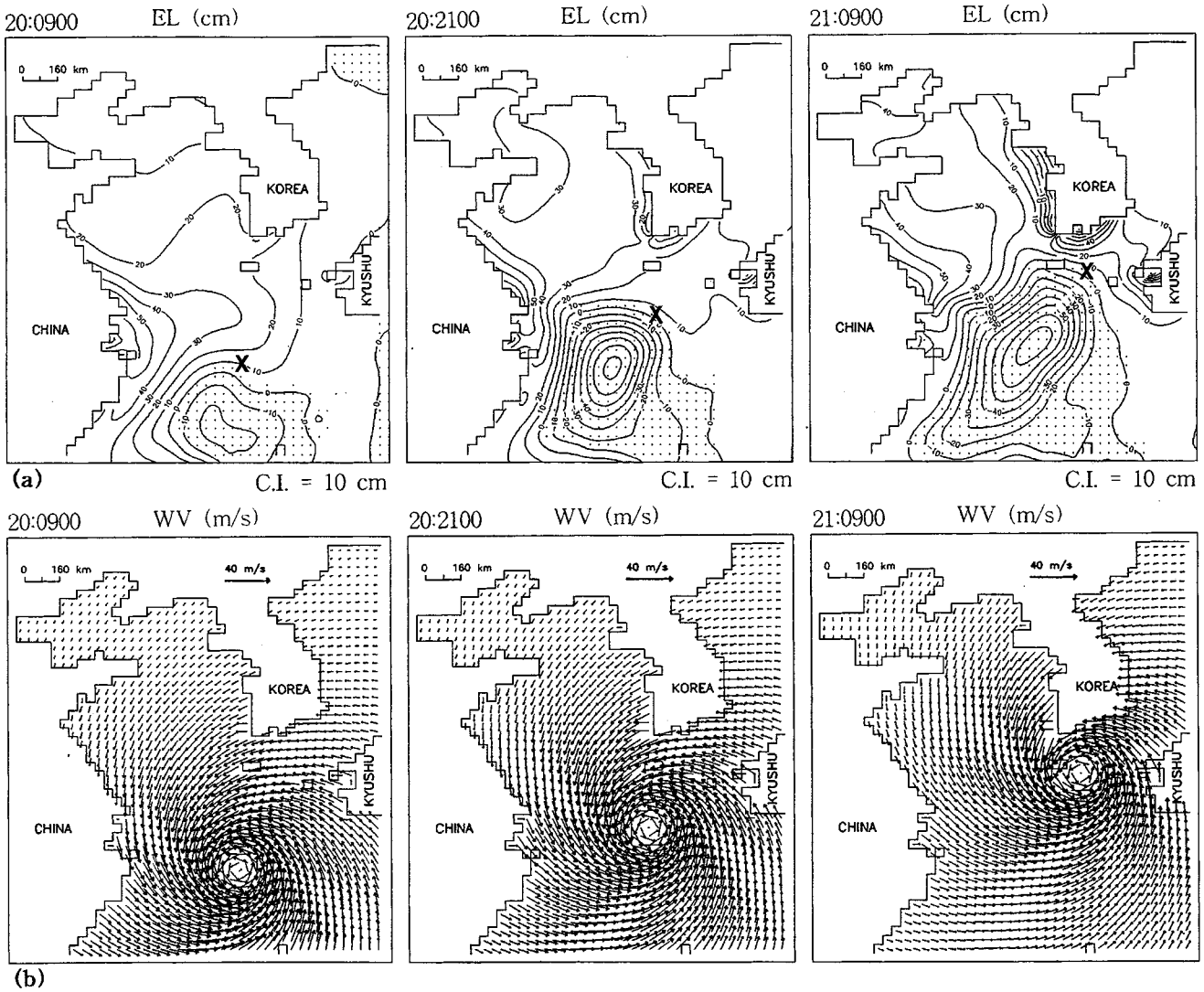

Fig. 7. The sea surface elevation a), wind vector b) from 20:0900 to 21:0900 with every twelve-hour. Shade zones represent negative sea level, and the center of the typhoon is marked by a cross symbol (×).

fields at 50 m and 80 m depths at 19:2100 (Fig. 9a) and 20:2100 (Fig. 9b) when the typhoon has been located at the southwest of Kyushu (see Fig. 5). In these periods, around St. T4 (black circle), there is no significant change of sea water properties in both layers in time. Temperature in the central area of the KS is near 18°C in 50 m and near 16°C in 80 m. Behind of the Tsushima Island, however, there is cold water lower than surrounding water, probably related to its topographic effect as discussed by Isoda (1989). At 21:0900 when the typhoon has entered the KS (Fig. 10a), in the upper layer (50 m), warm water over 20°C flows into the eastern channel (the upper panel). As seen in the velocity field (the lower panel), this warm water has been accompanied by the WKC mentioned in previous section. By passing of the typhoon (Fig. 10b), the WKC has more developed (the lower panel), resulting in increasing the transport of warm water (the upper panel). Thus, the model results show that a rapid increase of the observed temperature in the eastern channel can be explained by transport of warm water from the East China Sea, which is accompanied by the WKC. In the lower layer (80 m) at the same time (21:0900; Fig. 11a), temperature field (the upper panel) is still almost the same as before (see Fig. 10), despite that in the upper layer warmer water has been already transported, since the WKC does not yet develop at the lower layer (the lower panel). However, as it develops more (the lower panel in Fig. 11b), warm water higher than 18°C is transported into the eastern channel

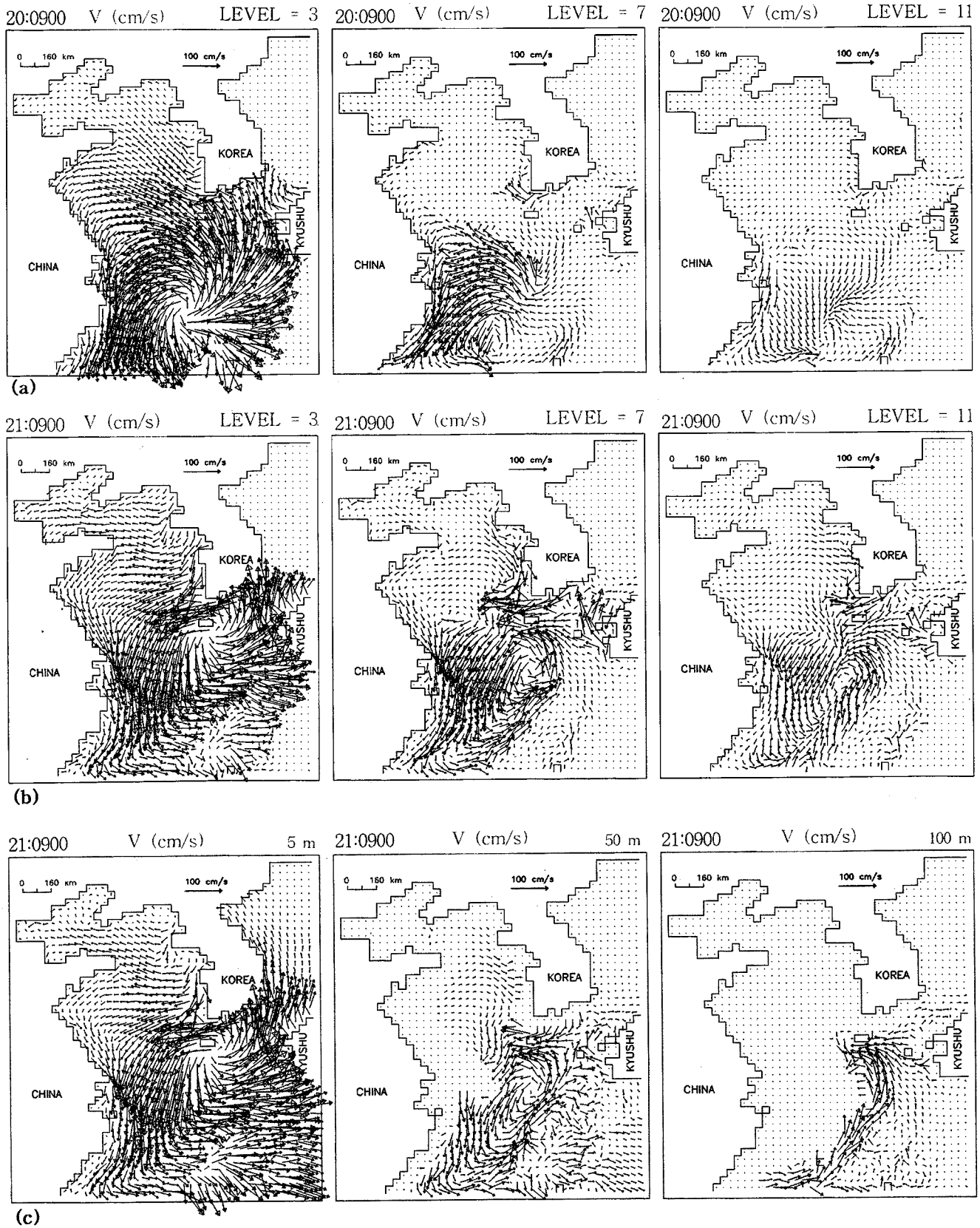

Fig. 8. The velocity field at 20:0900 a), at 21:0900 b), and in z-coordinate at 21:0900 c). They are given in three levels (levels 3,7, and 11).

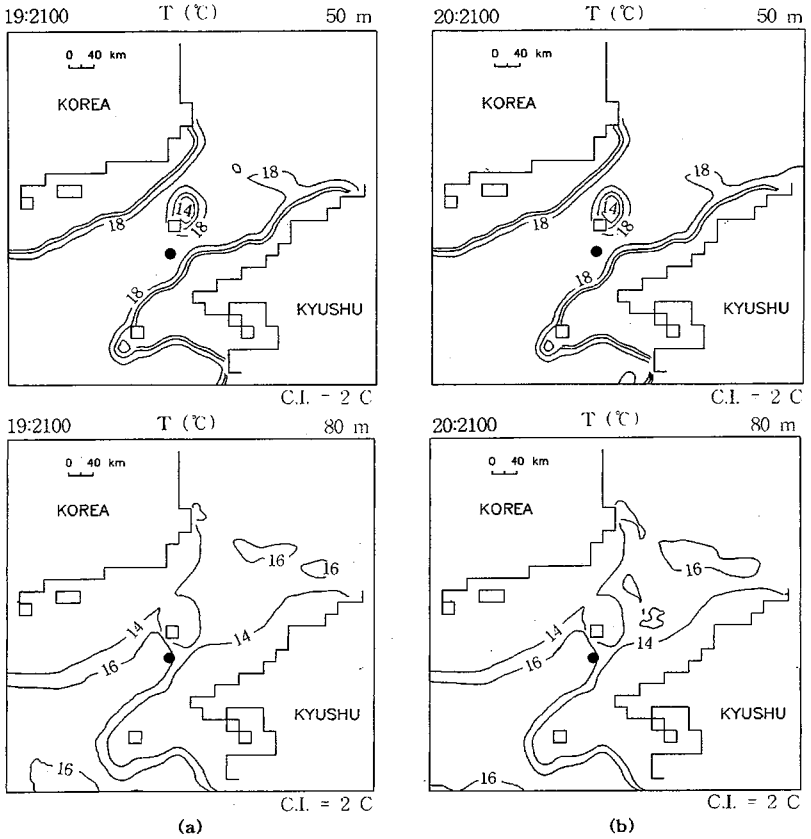

Fig. 9. Temperature fields at 50 m and 80 m depths at 19:2100 a), and at 20:2100 b). Contour intervals are 2°C. Black circles represent St. T4.

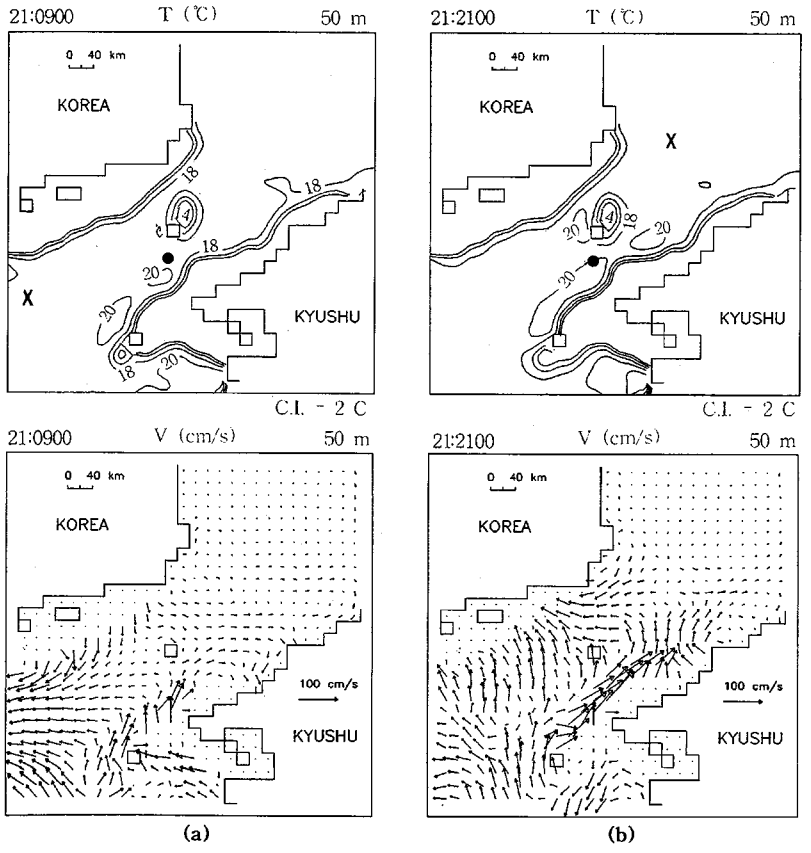

Fig. 10. Temperature (the upper panels) and velocity fields (the lower panels) at 50 m depth at 21:0900 a), and at 21:2100 b).

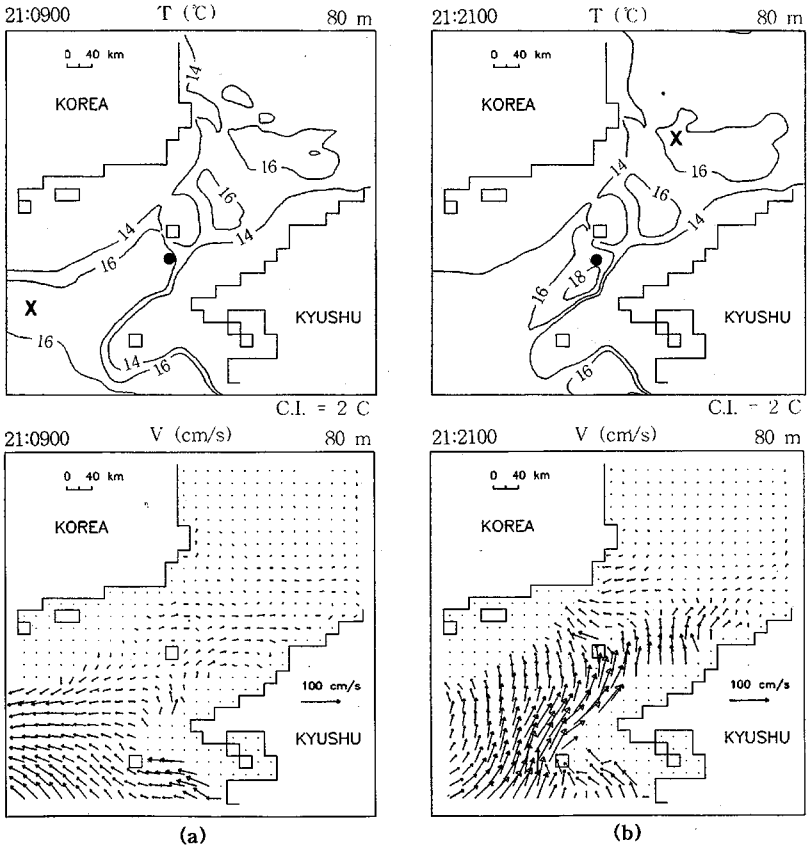

Fig. 11. Same as Fig. 10 except for 80 m depth.

(the upper panel in Fig. 11b). This result shows that a time lag of the maximum temperature in depth has been generated by difference of developing time of the WKC in depth.

Finally, we discuss about oscillation found in observed temperature and velocity fields after the passing of typhoon through the KS. Fig. 12 shows elevation fields from 22:0900 to 25:2100 with every 12-hour. After the typhoon enters the central of the East Sea (22:0900), some disturbance (positive sea level) propagates along the coast in the Yellow Sea and the East China Sea, and repeats from 25:2100 with a period of about 2.5-day as earlier indicated by HY. A space-time diagram of sea surface elevation is illustrated in Fig. 13 (see Fig. 4a for stations). A wave propagation is seen after the passing of typhoon through the KS (note that the period of the typhoon's passing is given by two horizontal bars). Its speed is about 20 m/s, and corresponds to the speed of Kelvin wave if we assume that the mean depth of the Yellow Sea is about 40 m. The periodicity of the oscillation, however, is not manifested compared with one obtained by HY. This will be discussed at next section. Consequently, the model implies that the oscillation in the observed temperature after the passing of the typhoon through the KS may be due to a basin-scale undulation with Kelvin wave although its periodicity is not clear.

CONCLUSION AND DISCUSSION

When typhoons (TP8305 and TP8410) passed around the KS, in the observation at St. T4 in the eastern channel corried out by Mizuno *et al.* (1986), we can find several oceanographic features; 1) the direction of the current was opposed to the northeasterly wind, 2) temperature rapidly increased having a time lag as the depth deepens, after then decreased with oscillation.

The POM version that incorporates a typhoon model reproduces the major features in the observation. In the model, the West Kyusyu Current (WKC), which flows northward along the west of Kyushu, plays important role in the oceanographic condition in the eastern channel in this period. This current is a coastal jet generated by an alongshore wind in the typhoon, and flows into the East Sea almost without regard to the wind field within the KS in this period. Warm water from the East China

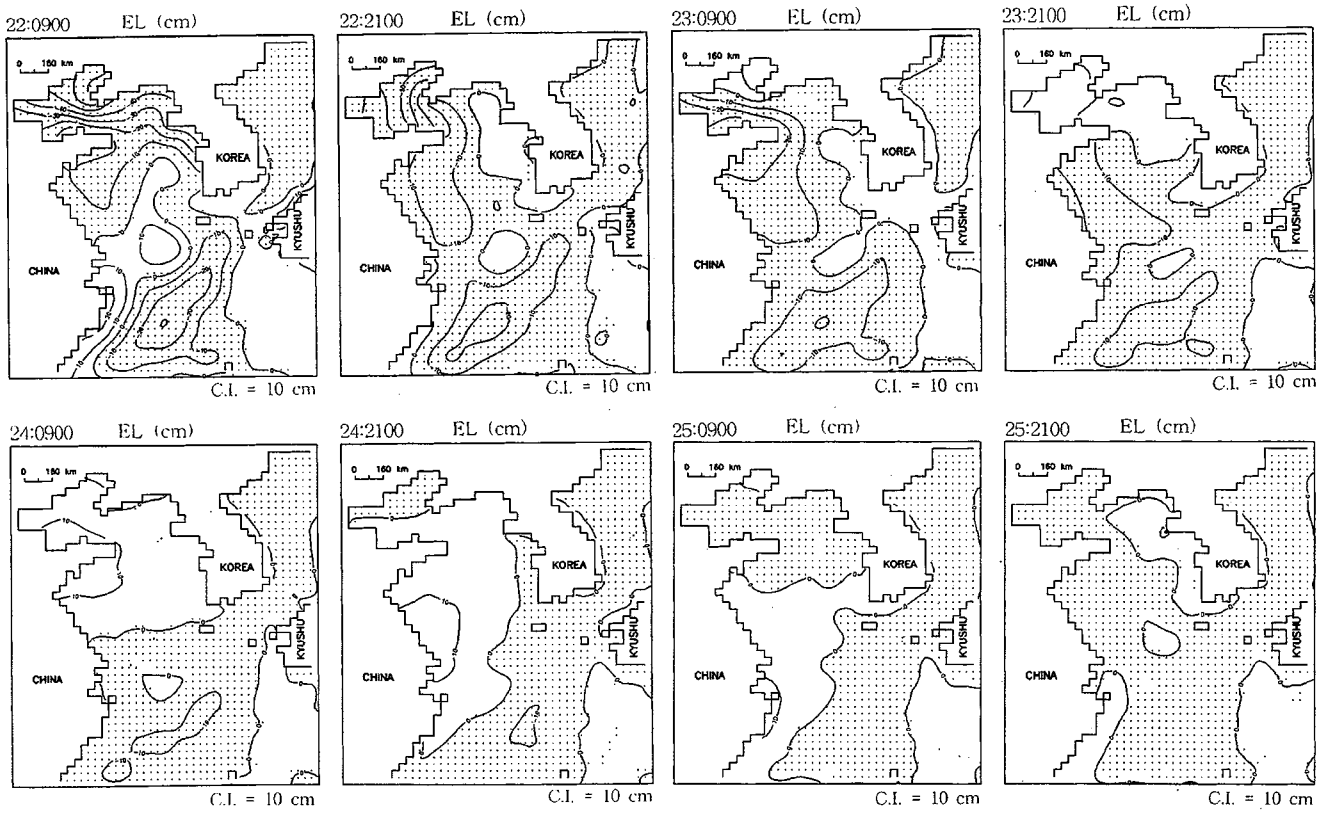

Fig. 12. Elevation from 22:0900 to 25:2100 with every twelve-hour.

Sea is transported by the WKC into the eastern channel, resulting in a rapid increase of the temperature. The WKC first has developed at the surface layer, and gradually at the lower layers in time. This caused a time lag in temperature increase in depth (Figs. 2 and 3).

In addition, elevations and velocities in the case of TP8305 (Fig. 14) were obtained using a numerical shallow water model under the same conditions as the typhoon parameters (e.g., Cd etc.) in the present study with an extended study area. At 16:2100 (Fig. 14a) and 17:0900 (Fig. 14b) in August, 1983 when the typhoon (cross mark) hit the south of Japan, it is seen that as the case of TP8410, the WKC also flows into the eastern channel, and continues to flow along the northern Japanese coast. The strong current, more than about 10 cm/s as a mean velocity, flowing into the eastern channel at 17:0900 (Fig. 14b) is well identified by the observation as shown in Fig. 2. In this case, the WKC develops accompanied by a Kelvin wave along the coast in the south of Japan. Consequently, this paper indicates that when typhoons pass around the KS, oceanographic condition in the KS should be greatly influenced with the WKC. The strength of

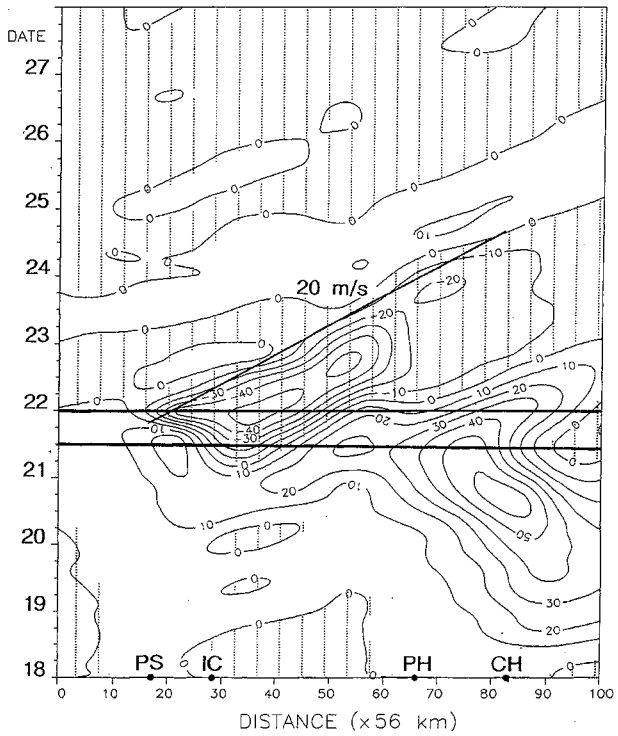

Fig. 13. A space-time diagram of sea surface elevation. See Fig. 4a for stations. The period (twelve-hour) of passing of typhoon is given by two horizontal bars. Shade zones represent negative sea level. A roughly propagation speed of wave is given by 20 m/s.

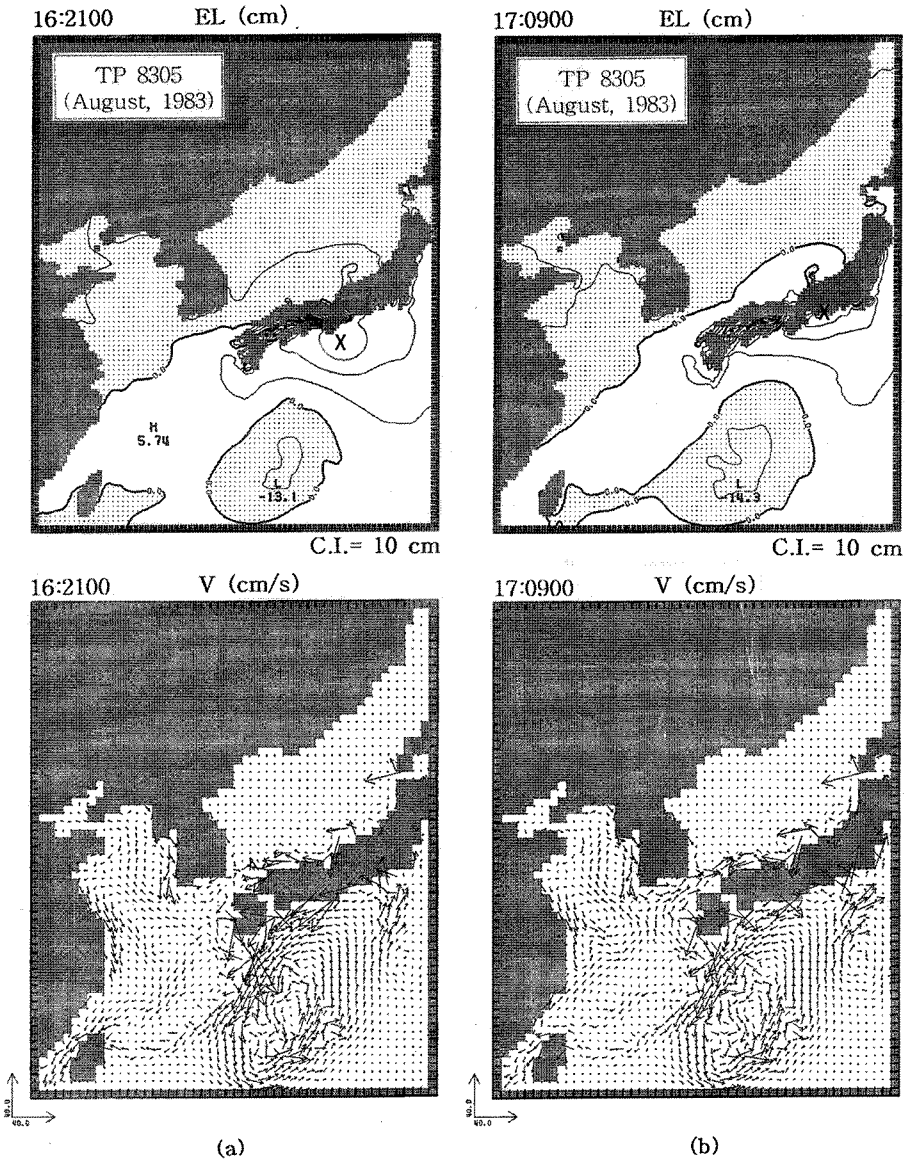

Fig. 14. Elevation (the upper panels) and velocity (the lower panels) at 16:2100 a), and at 17:0900 b), August, 1983 when typhoon TP8305 (cross mark) hit the south of Japan. These results were obtained using a numerical shallow water model.

the WKC should be primarily associated with the track of typhoon since it is generated by alongshore wind in the west of the Kyushu (or in the south of Japan, see Fig. 14). For example, a typhoon which moves towards the China will be difficult to generate and develop the WKC although we here did not examine it. Tracks of the typhoons presented here, TP8305 and TP8410, are likely preferable to generating and developing the WKC.

In this paper, we pointed out several oceanographic features in velocity and temperature field (Figs. 2 and 3) in the observation carried out by Mizuno *et al.* (1986), and in the model this phenomena were generated by the West Kyushu Current. The existence of this current, however, was not identified yet by the observation.

In the model, oceanographic conditions in the KS, such as velocity and temperature distributions, have been greatly changed by typhoons even for several days, and in particular affected by the WKC resulting in more warming sea water in the eastern channel than in the western channel (Fig. 9). In this effect, the WKC probably would contribute in part to causing difference of sea water properties between two channels of the KS mentioned by many authors (Omura *et al.*, 1994; Isobe, 1994; Hong, 1998c).

The model has been much simplified to capture only basic key points. The basic currents, such as the Tsushima Current, has been neglected, and would result in modifying somewhat strength of the current in the eastern channel. This current,

however, would act on intensifying the WKC. For a goal of this paper, the model region has been cut off a lot of the East Sea, so that in the East Sea activity of many eddies generated by the typhoon (see HY) has been negligible, although this paper does not focus on it. This would affect periodicity of a basin-scale undulation (Fig. 13) since this undulation is related to the scale of the basin in the model. In the model, we also simply initialized horizontally homogeneous temperature field at some levels without considering different temperature in each region, so that it will somewhat modify the calculated temperature field in the vertical. This must be complemented in the future.

ACKNOWLEDGMENTS

The author would like to thank Dr. H. M. Lee of Pukyong National University for valuable comments. He also wishes to acknowledge the financial support of the Korea Research Foundation in the program year of 1997, and this study was also supported in part by the Korea Science and Engineering Foundation (KOSEF) through the Research Center for Ocean Industrial Development (RCOID) of Pukyong National University.

REFERENCES

Blumberg, A.F. and G.L. Mellor, 1983. Diagnostic and prognostic numerical circulation studies of the South Atlantic Bight. *J. Geophys. Res.*, **88**: 4579–4592.

Blumberg, A.F. and G.L. Mellor, 1987. A description of a three dimensional coastal ocean circulation model. In: Three Dimensional Coastal Ocean Models, Coastal Estuarine Science, 4th ed., edited by Heaps, N.S., American Geophysical Union, Washington D.C., pp. 1–16.

Fujita, T., 1952. Pressure distribution within typhoon. *Geophys. Mag.*, **23**: 437–451.

Galperin, B., L.H. Kantha, S. Hassid and A. Rosati, 1988. A quasi-equilibrium turbulent energy model for geophysical flows. *J. Atmos. Sci.*, **45**: 55–62.

Galperin, B. and G.L. Mellor, 1990a. A time-dependent, three-dimensional model of the Delaware Bay and River. Part I. Description of the model and tidal analysis. *Estuar. Coast. Shelf Sci.*, **31**: 231–253.

Galperin, B. and G.L. Mellor, 1990b. A time-dependent, three-dimensional model of the Delaware Bay and River. Part 2. Three dimensional flow fields and residual circulation. *Estuar. Coast. Shelf Sci.*, **31**: 255–281.

Hong, C.H. and J.H. Yoon, 1992. The effect of typhoon on the sea level variations in the Tsushima Current (in Japanese). *J. Oceanogr., Umino Kenkyu*, **1**: 225–249.

Hong, C.H. and J.H. Yoon, 1993. The response of sea levels to typhoons in the Japan Sea. Part I. The response on the north Japanese coast. *Bull. Korean Fish. Soc.* **26**: 567–579.

Hong C.H., 1996. Sea level response in the Korea Strait to typhoons. *J. Korean Soc. Oceanogr.*, **31**: 107–116.

Hong, C.H. and Y.K. Choi, 1997. The response of temperature and velocity fields to M2 tide in the Deukryang Bay in the southern sea of Korea. *J. Korean Fish. Soc.*, **30**: 667–678.

Hong, C.H., 1998a. Simulation of sea water response in Deukryang Bay to typhoon using the Princeton ocean model. *J. Korean Soc. Oceanogr.*, **33**: 53–63.

Hong, C.H., 1998b. On the circulation in the Jinhae Bay using the Princeton ocean model. I. Characteristics in vertical tidal motion. *J. Fish. Sci. Tech.*, **1**: 168–179.

Hong, C.H., 1998c. A relationship between the sea level variations in the Korea Strait and the Tokara Strait in the Kuroshio region. *J. Fish. Sci. Tech.*, **1**: 113–121.

Isoda, T., 1989. Topographic effects on the Tsushima Islands on the Tsushima Warm Current. *Bull. Coast. Oceanogr.*, **27**: 76–84.

Isobe A., 1994. Seasonal variability of the barotropic and baroclinic motion in the Tsushima-Korea Strait. *J. Oceanogr.*, **50**: 223–238.

Mellor G.L., 1996. Users guide for a three-dimensional, primitive equation, numercial ocean model. Atmospheric and Oceanic Science Program, Princeton University, 39 pp.

Mizuno S., K. Kawatate, and T. Miita, 1986. Current and temperature observations in the east Tsushima Channel and the Sea of Genka. *Prog. Oceanogr.*, **17**: 277–295.

Miyazaki, M., T. Ueno, and S. Unoki, 1961. Theoretical investigation of typhoons surges along the Japanese coast. *Oceanogr. Mag.*, **13**: 51–75.

Oh I.S. and D.E. Lee, 1998. A numerical study on 3 dimensional circulation in the Yellow and East China Seas. Abstract in J. Korean Soc. Oceanogr. Autumn meeting, p 456.

Oey, L.Y., G.L. Mellor, and R.I. Hires, 1985a. A three-dimensional simulation of the Hudson Raritan estuary. Part I. Description of the model and model simulations. *J. Phys. Oceanogr.*, **15**: 1676–1692.

Oey, L.Y., G.L. Mellor, and R.I. Hires, 1985b. A three-dimensional simulation of the Hudson Raritan estuary. Part II. Comparison with observations. *J. Phys. Oceanogr.*, **15**: 1693–1709.

Oey, L.Y., G.L. Mellor, and R.I. Hires, 1985c. A three-dimensional simulation of the Hudson Raritan estuary. Part III. Salt flux analysis. *J. Phys. Oceanogr.*, **15**: 1711–1720.

Omura K., and K. Kawatate, 1994. Hydrographic features of the bottom cold water in the west Tsushima channel (in Japanese). *Bull. Fukuok Fish. Mar. Tech. Res. Cent.*, **2**: 93–101.

Yi S. U., 1974. Variations of oceanic condition and mean sea level in the Korea Strait. In: The Kuroshio, edited by Marr, J. C., East-West Center Press, Honolulu, pp. 125–141.

Manuscript received March 4, 1999
Revision accepted June 3, 1999